Supplementary Information

In situ, real-time tracking of cell wall topography and nanomechanics of antimycobacterial drugs treated *Mycobacteria JLS* using atomic force microscopy

Yangzhe Wu, Anhong Zhou *

Biological Engineering Program, Utah State University, 4105 Old Main Hill, Logan, Utah 84322-4105

*Email address: Anhong.Zhou@usu.edu

Experimental procedure

Mycobacterium JLS culture

The *mycobacterium* sp. strain JLS (*M. JLS*) was obtained from Dr. Ronald Sims' and Dr. Charles Miller's laboratories at the Department of Biological and Irrigation Engineering at Utah State University (Logan, Utah). The cells were cultured in LB broth composed of yeast extract, peptone from casein, and sodium chloride (mass ratio, 1:2:1) at room temperature by the normal shaking method. Because of their robust and thick cell walls, mycobacteria have a very low permeability to nutrients and therefore grow very slowly [1]. One week growth time was needed prior to AFM observation.

Bacteria sample preparation

We found that the hydrophobic property of living *M. JLS* cells can make itself stably attached onto the Petri dish (hydrophobic polystyrene) without use of any cross-linker agents; therefore, this very simple and efficient approach avoids the potential surface structure rearrangement or denaturation due to cross-linker treatment and allows bacteria cells maintain native hydrated state during AFM measurement. The detailed preparation procedures are 1) 1 ml of bacteria solution were then centrifuged at 2500 rpm for 2 min (Eppendorf Minispan), and then the supernatant was discarded; 2) the bottom pellet was re-suspended and about 0.5 ml of bacteria suspension was dropped onto Petri dish (3 cm in diameter) and let it stand by approximately 10

min; 3) then the Petri dish containing bacteria cells was gently rinsed with de-ionized water twice to remove un-attached bacterial cells; 4) about 2 ml LB broth containing ethambutol (EMB) ($C_{10}H_{24}N_2O_2$, M.W. 204.31) (10 µg/ml) or isoniazid (INH) ($C_6H_7N_3O$, M.W. 137.14) (10 µg/ml) was added into Petri dish. Finally, the Petri dish was then immediately transferred to AFM scanner stage for the measurements. The sample preparation is described schematically in Fig. s1. In our experiments, by referring its minimal inhibitory concentration (MIC) to *Mycobacterium bovis BCG* [2] and to other *Mycobacterium* strains [3], and considering that to induce visible alterations under AFM in several hours, 10 µg/ml of EMB dissolved in LB broth medium was used to treat *M. JLS*. For the comparison purpose, the concentration of INH in LB broth medium was also at 10 µg/ml. All AFM measurements were conducted in LB medium at ambient room temperature.

In addition, it should be noted that, it would take more than 30 min to obtain the first AFM image.

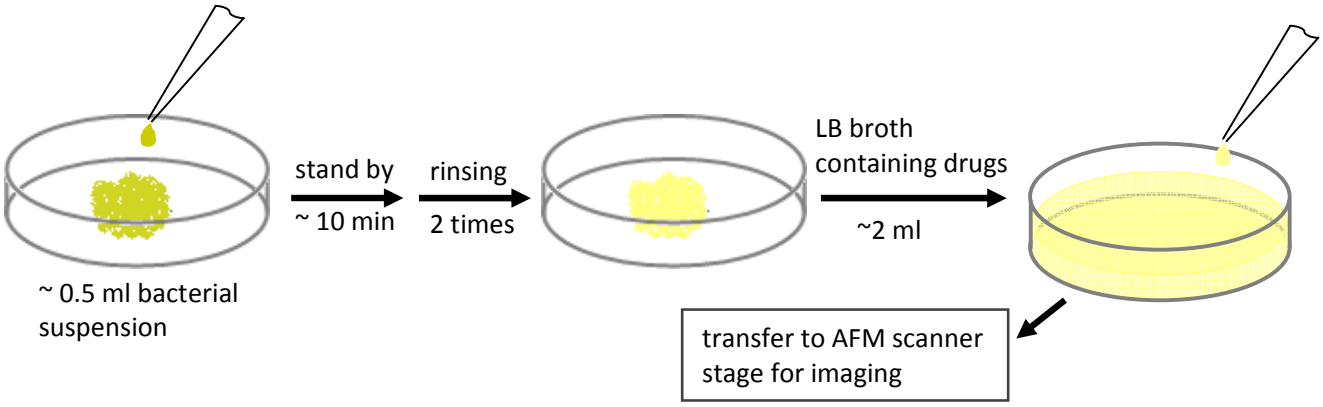

Figure s1. Schematic illustration of bacteria sample preparation for AFM measurements.

Atomic force microscopy measurements

The PicoPlus AFM (Agilent Technologies, U.S.A) was controlled by software PicoScan 5.4 (Agilent Technologies U.S.A.). Contact mode is used throughout the experiments. The spring constant of the cantilevers (Veeco Inc, U.S.A.) used in the experiments was 0.32 N/m. The cantilever length was 0.4~0.7 µm, and the curvature radius of the Si_3N_4 tip was approximate 10 nm. The values of adhesion force were extracted from deflection (nm) vs. distance (nm) curves

via the software Scanning Probe Image Processor (SPIP) (Image Metrology, Denmark). The histograms were drawn using OriginPro 7.5 (OriginLab Corp., USA).

Calculation of bacterial spring constant (k_b)

By utilizing the contact AFM, hundreds of deflection-force curves of each time point were acquired. In the process of the AFM tip approaching sample surface, the elasticity of cell wall can be evaluated based on the slope of compliance portion of deflection-force curve. Here, according to the calculation formula (1) proposed by literatures [4, 5], the bacterial spring constants were correspondingly calculated.

$$k_b = -k_c \frac{s}{1+s} \qquad (1)$$

Where, **s** is the value of the linear slope of approaching branch, the ratio of *deflection (nm)* to *distance (nm)*; k_b and k_c represent the spring constants of the bacterial cell wall and the cantilever, respectively.

Calculation of bacterial Young's modulus

If assuming that both bacterium and cantilever can be modeled as springs, then both of them can move in the process of force acquiring, therefore, they can be treated as two springs connected in series. Therefore, the effective spring constant of cantilever is:

$$\frac{1}{k_{eff}} = \frac{1}{k_b} + \frac{1}{k_c} \qquad (2)$$

Where, k_b is bacterial spring constant; k_c, spring constant of cantilever; k_{eff}, effective spring constant of cantilever.

Then, the loading force of AFM probe approaching onto cell surface is:

$$F_{loading} = k_{eff} * D \qquad (3)$$

Where, $F_{loading}$ is the loading force; **D,** cantilever deflection (nm).

If assuming the tip possesses a paraboloidal shape with a tip apex *R*, then Young's modulus can be obtained according formula (4) that has been widely accepted:

$$F(\Delta z) = \frac{4\sqrt{R}\,E_{cell}}{3\,(1-\eta_{cell}{}^2)}\,\Delta z^{1.5} \qquad (4)$$

Where, $\boldsymbol{R}$ is tip apex (curvature radius); $\boldsymbol{E_{cell}}$, Young's modulus; $\boldsymbol{\eta_{cell}}$, Poisson ratio (assuming 0.5); $\boldsymbol{\Delta z}$, indentation.

Here we only calculate average Young's modulus for each time point of measurement. At each time point of force curves acquiring, we averaged the slope of hundreds of curves; then we selected a curve with the value of average slope, which then was used to calculate the Young's modulus. The statistical data were reported as mean±SD (standard deviation).

Graphing of adhesion force mapping and bacterial spring constant mapping

The mapping of adhesion force or bacterial spring constant is graphed by adjusting original measured values by log(original value+1)×scale, scale is usually a number like 160 or 256, or even larger, depending on the original value. But for one parameter mapping, the same scale value is used to adjust the original values. Then the re-scaled data are plotted with a color map with 256 numbers of colors by Matlab program version R2009a (MathWorks, Inc.).

Continuous measurements of EMB-*mycobacterium* interaction

Real-time tracking of topography changes

Figure s2 presents serial deflection images of living *M. JLS* cells acquired in LB broth medium containing 10 μg/ml of EMB. The time had elapsed 80 min when the first image (a) was obtained. Bacteria didn't begin to shrink until more than 8 hours of EMB-*M.JLS* interaction, and this shrinkage became more evident in image (j) (the upper cell pointed by black arrow). AFM images (k, l, m) depict that bacterial collapse occurred in a very short time (within 20 min). When tip scanned across the line pointed by white arrow from upper to bottom (k, l) or from bottom to upper (m), cell wall collapse occurred. The similar phenomenon was also observed in the following measurement (see Fig. s4-d). Image (n) indicates the collapsed cells were eventually removed due to the lost of cell walls. In addition, though the convolution artifacts are visible (asterisk, Fig. s2-a), it did not affect our analysis of time lapse deflection images. The tip

convolution artifacts occur often in visualization of cell topography[6-8]. These convolution artifacts appeared as well in the following cell observation (see Fig. s4-a, asterisks highlighted).

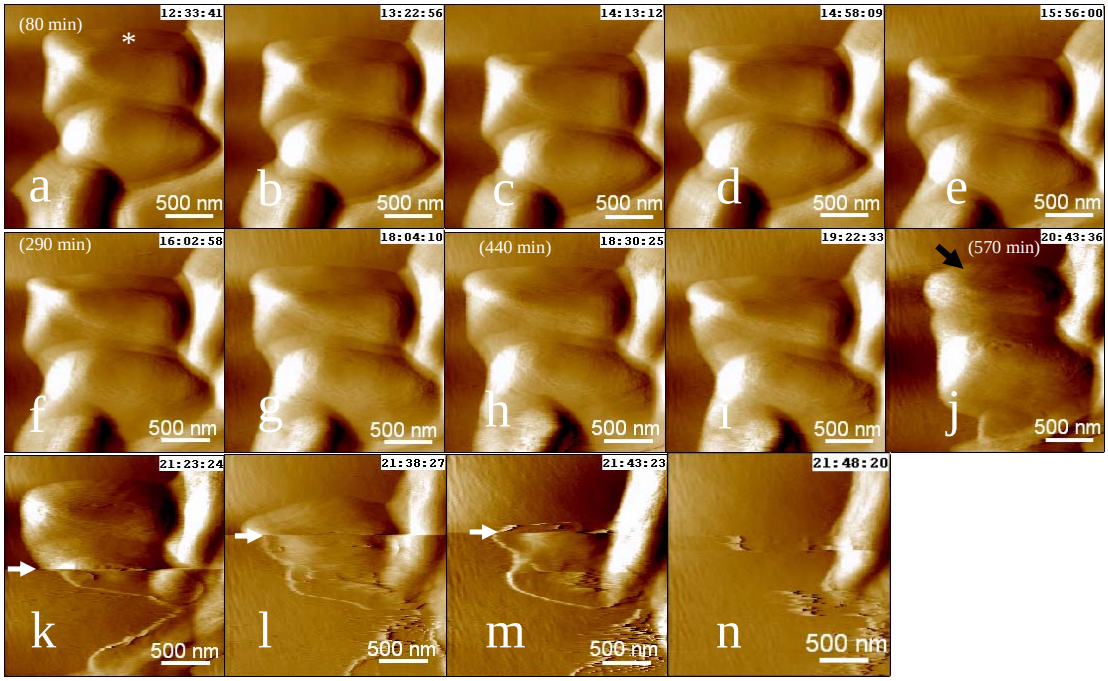

Figure s2. Deflection images of *M. JLS* cells acquired in LB broth medium containing EMB (10 µg/ml). The serial images indicate that the observed two cells did not change obviously from (a) to (h); however, image (i) shows the starting of shrinking and this shrinkage became more evident in image (j) (the upper cell pointed by black arrow). Image (k) records the lower cell is in collapse, and images (l, m) depict these two cells collapsed wholly; white arrows in (k-m) show the moments of collapse occurring. (n) shows collapsed cell fragments were removed by the scanning tip.

Nano-biomechanical properties mapping and cell height profiles

The representative topography images of Fig. s3(a,b,c,d) correspond to the deflection images Fig. s2(a,f,h,j), respectively. The statistical results of nano-biomechanical properties including adhesion property (F) and bacterial spring constant (k_b) are shown in Fig. s3(e-h, i-l). Because of the individuality and the different growth phases of each bacterial cell, the cell topography alters differently from each other and cell collapse would occur at the different time. With the lapse of EMB-bacteria interaction time, the adhesion force (F) decreased dramatically (>5%), from 0.29 nN (Fig. s3e, 80 min) to 0.19 nN (Fig. s3h, 570 min).

As for bacterial spring constant (k_b), its histogram distribution presents two populations (Fig. s3-i, j, k) before cell collapse, including one smaller population at 0.16 N/m; in contrast, the smaller

population disappeared after cell collapse (l). Moreover, the collapse leads to a decrease in k_b about ~0.02 N/m from 0.085 N/m (Fig. s3k, 440 min) to 0.065 N/m (Fig. s3l, 570 min).

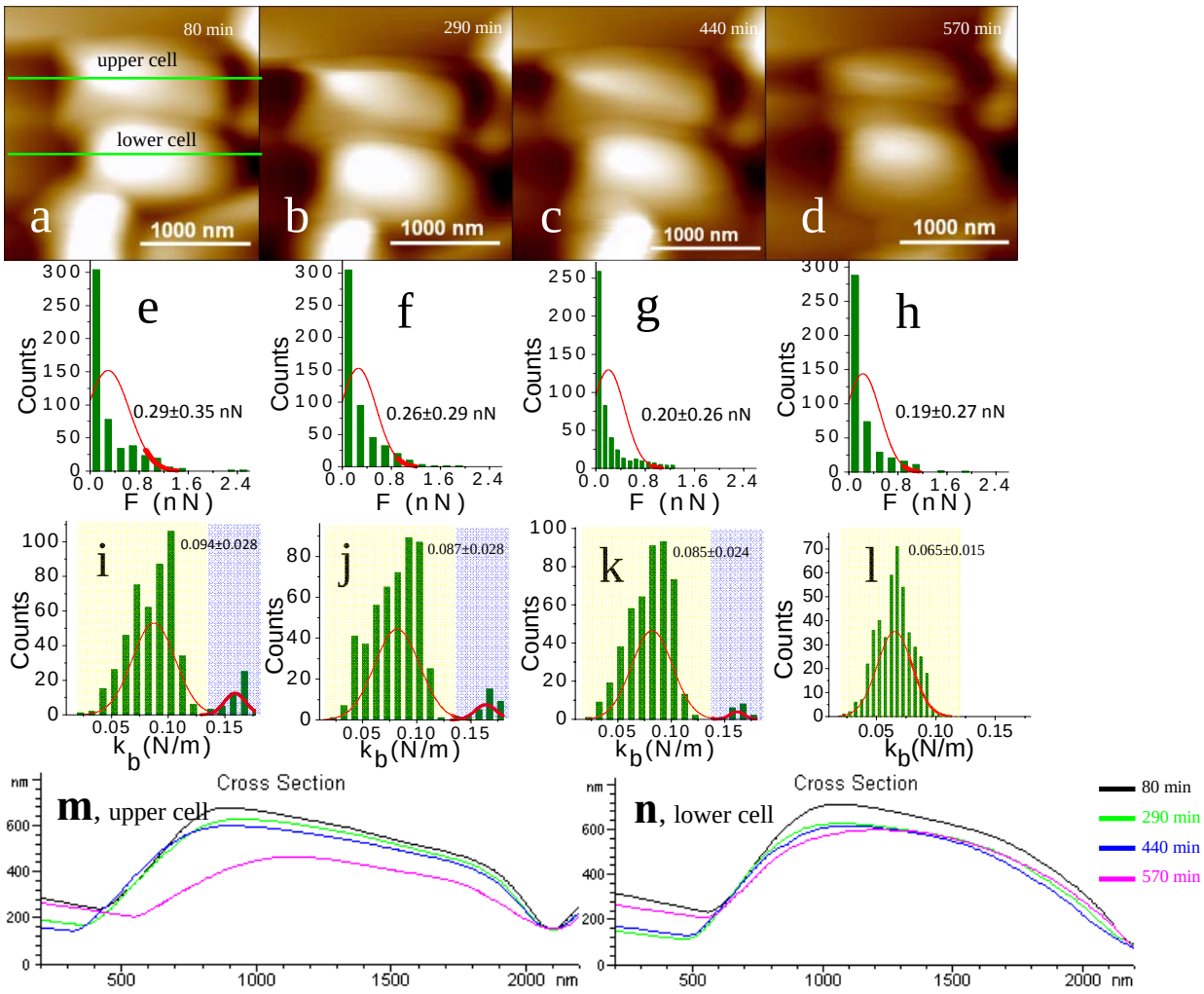

Figure s3. Representative images of *M. JLS* cells interacted with EMB (10 μg/ml) over interaction time intervals at 80 min, 290 min, 440 min, and 570 min.. (a-d) Topographies of M. JLS, corresponding to the deflection images Fig. s2(a,f,h,j), respectively; (e-h) adhesion force distribution; (i-l) bacterial spring constant (k_b) distribution. (m, n) the comparison of cross section profiles as crossed by the green lines on the two cells in (a).

Images (m, n) are cross section profiles acquired from topographies (a-d) that exhibit the topography changes over interaction time, which clearly illuminates the variation and individuality of each observed cell. As for the same interaction time, the upper cell (m) shrinking occurs faster than the lower cell (n). It is interesting to note that, though the cell height decreased over the interaction time, the cross section profiles remain relatively smooth, indicating EMB doesn't directly attack the cell outer layer.

Continuous measurements of INH-*mycobacterium* interaction

Real-time tracking of topography changes

Figure s4 displays the serial deflection images of living *M. JLS* cells interacted with 10 μg/ml of INH in LB broth medium. It should be noted that, when the first image (a) was captured, the cells have been in cell division with the appearance of a characteristic septum. The white arrows in (a, b) indicate the septum furrow, showing that the cell is in division. The dividing cells are going to further proceed to the division process (c). Image (d) indicates the moment at which the cell collapse occurs, when tip scanned from bottom to top across the line pointed by white arrow. In the subsequent scanning from top to bottom (e), the lower half of the cells shrinks to the same size as the upper half. This shrinkage continues in the following scanning from (f) to (j). Consequently, cell height decreases gradually from (e) to (g) (see Fig. s5-p); however, the decreasing magnitude did not alter dramatically from (g) to (j) according to measurements. In this experiment, it is very interesting to capture a bacterial cell in division and observe its dynamic change in topography induced by drug interaction. It is evident that the division process is effectively inhibited (a-d), even the cells try to divide and separate each other into two daughter cells at (c). The shrinking and eventually collapse of the cells in presence of INH over the time are resulted from the attack of INH to the cell wall component, mycolic acid (see Fig. 1), and this attack makes the lost of cell rigidity. Fig. s2 and Fig. s4 show the dynamic observations of the interaction between different drugs and mycobacterial cells that are in different cell division stages: the cells captured in Fig. s4 have been dividing (indicative of septum structure) when they were first captured; while the cells in Fig. s2 may be in the early stage of cell division or the division process hasn’t been started yet (no septum is observed).

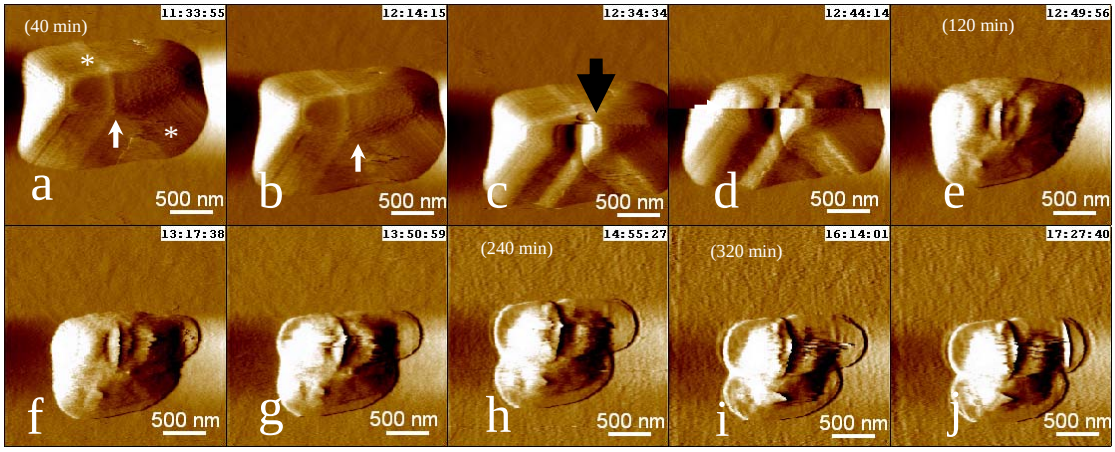

Figure s4. Deflection images of *M. JLS* cells acquired in LB broth medium containing INH (10 µg/ml). The serial images indicate that the observed cell topography did not change obviously from (a) to (b), instead the presence of septum furrow structure. Cell collapse occurred at the moment when tip scanned across the line pointed by white arrow from bottom to top (d). Measurements indicated that cell height gradually decreased from (e) to (g); however, cell topography and the height did not alter dramatically from (g) to (j). The black arrow in image (c) points the cleft position, displaying the septum furrow correlated with bacterial division.

Nano-biomechanical property mapping and cell height profiles

Similarly, adhesion property (F) and bacterial spring constant (k_b) are used to assess the cell biomechanic changes of *M. JLS* cells over the time of interaction with INH. The results are shown in Fig. s5. The representative topography images of Fig. s5(a,b,c,d) correspond to the deflection images Fig. s4(a,e,h,i), respectively. Similar to EMB treated M. JLS, with lapse of INH-bacteria interaction time, the adhesion force decreased apparently (Fig. s5, e-h) (>5%), from 2.79 nN to 0.46 nN, during the entire period of measurement (320 min). In contrast, the bacterial spring constant (k_b) decreased to the half in the first 120 min of observation, from 0.161 N/m (I, 40 min) to 0.074 N/m (j, 120 min); and then it remained stable at the level of 0.08 N/m (k-l), after cell wall collapse occurred at 120 min (b). The increases in k_b from 0.074 N/m (j, 120 min) to 0.089 N/m (l, 320 min) might come from the contribution of the substrate (very flat cell body residual after collapsed). The small population of k_b distribution observed in (i) disappeared in (j-l). Fig. s5p displays the variation of cell height from cross-section profiles measured from images (a-d), showing the cell height of shrinking cells decreases as well.

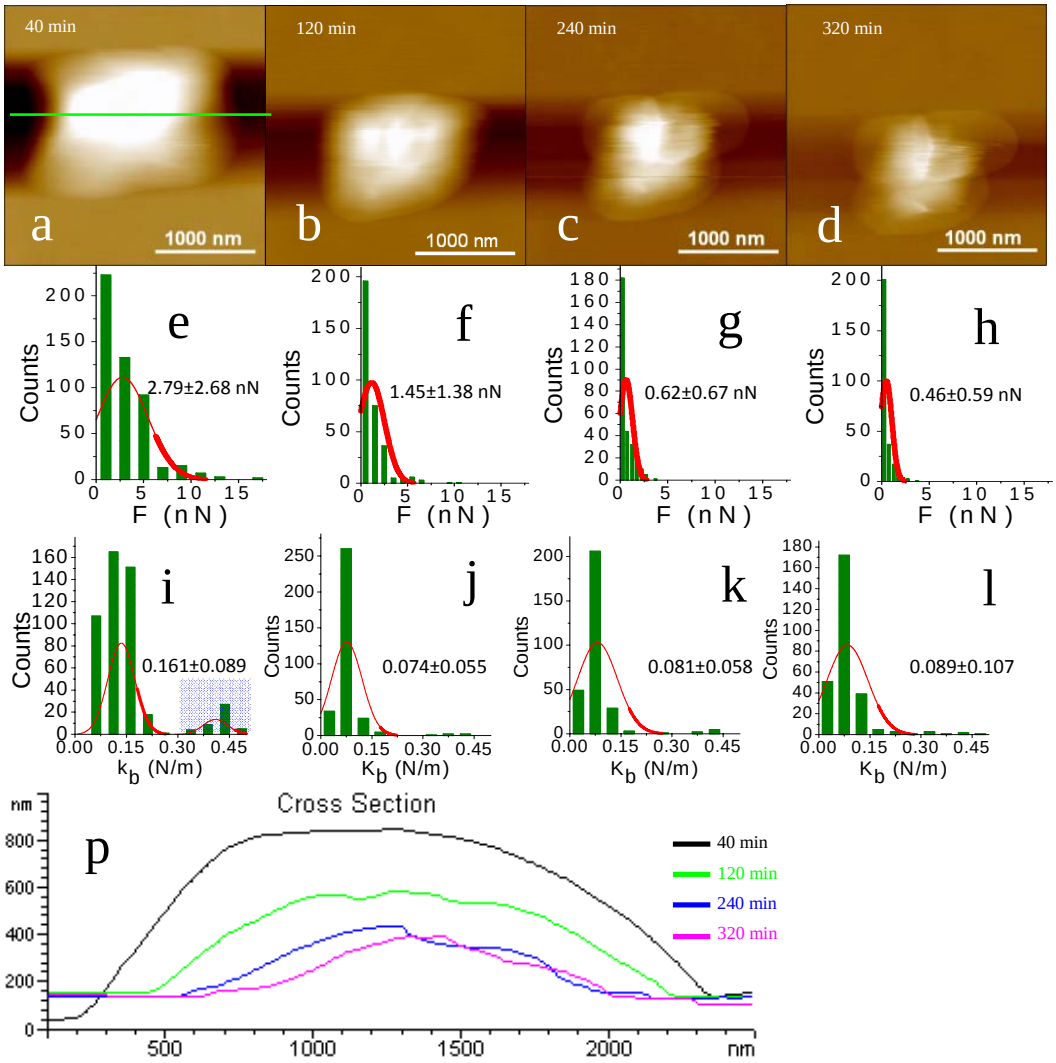

Figure s5. Representative results of *M. JLS* cells interacted with INH (10 μg/ml) over interaction time intervals at 40 min, 120 min, 240 min, and 320 min. (a-d) Topographies of *M. JLS* cells interacted with INH, corresponding to Fig. s4(a,e,h,i), respectively; (e-h) adhesion force distribution; (i-l) bacterial spring constant (k_b) distribution; (p) Comparison of cross section profiles as crossed by the green lines in (a).

According to the measurements, we found that though the two drugs (EMB, INH) target the different cell components, the induced changes in topography and biomechanical properties before and after cell wall collapse occurring are similar: 1) cell wall collapse occurs; 2) cell wall surface maintains smooth throughout the observation time; 3) decreases in adhesion force and k_b; 4) k_b distribution altered from two populations before cell collapse to one population after collapse; 5) drugs inhibit the further division of dividing cells.

References

1. M. Daffe and J. M. Reyrat, *The Mycobacterial cell envelope*, ASM Press, Wanshington, DC, 2008.
2. C. Verbelen, V. Dupres, F. D. Menozzi, D. Raze, A. R. Baulard, P. Hols and Y. F. Dufrene, *FEMS Microbiology Letters*, 2006, **264**, 192-197.
3. D. Lechner, S. Gibbons and F. Bucar, *Phytochemistry Letters*, 2008, **1**, 71-75.
4. S. B. Velegol and B. E. Logan, *Langmuir*, 2002, **18**, 5256-5262.
5. M. Arnoldi, M. Fritz, E. Bauerlein, M. Radmacher, E. Sackmann and A. Boulbitch, *Physical Review E*, 2000, **62**, 1034-1044.
6. Y. F. Dufrene, *Nat Protoc*, 2008, **3**, 1132-1138.
7. G. Francius, B. Tesson, E. Dague, V. Martin-Jezequel and Y. F. Dufrene, *Environ Microbiol*, 2008, **10**, 1344-1356.
8. S. B. Velegol, S. Pardi, X. Li, D. Velegol and B. E. Logan, *Langmuir*, 2003, **19**, 851-857.